JPL

The Nanoelectronic Modeling Tool (NEMO) and its Expansion to High Performance Parallel Computing

Gerhard Klimeck

Jet Propulsion Laboratory

California Institute of Technology

Chris Bowen, Tim Boykin[1], Fabiano Oyafuso[2], Carlos H. Salazar-Lazaro, Adrian Stoica, and Tom Cwik

Jet Propulsion Laboratory/California Institute of Technology

[1)]University of Alabama in Huntsville

[2)]University of Illinois

Outline

- NEMO genealogy and general features
- Structural device optimization:
  - Massively parallel genetic algorithm package
- Full band transport simulations:
  - Electron transport
  - Hole transport
- Comparison between k.p and sp3s*
- Conclusion

NEMO Genealogy

- NEMO was developed under a government contract at Texas Instruments and Raytheon from 1993-1997
  - Theory
    - Roger Lake, Chris Bowen, Tim Boykin (UAH), GK
  - Graphical User Interface
    - Dan Blanks, GK
  - Programming Approach, Philosophy, and Prototypes
    - Bill Frensley (UTD), GK
  - Coding
    - Manhua Leng (UTD), Chenjing Fernando, Paul Sotirelis, Dejan Jovanovic, Mukund Swaminathan (UTA), GK
  - Experiments for verification
    - Ted Moise, Alan Seabaugh, Tom Broekaert, Berinder Brar, Yung-Chung Kao

- NEMO is based on non-equilibrium Green functions, in an implementation that is novel. The development of NEMO has benefited from the vast research on resonant tunneling diodes that had been done before the project.

Summary of NEMO Capabilities

- Interface / Users:
  - FAST and dirty design. interactive
  - Comprehensive analysis (SLOW). batch
- Physics
  - Charging
    - Semi-classical self-consistency, quantum self-consistency
  - Scattering
    - Phonons, alloy disorder and interface roughness (1band)
  - Bandstructure
    - 1, 2, 10 tight binding band models nearest and next nearest neighbor coupling.
  - Realistically long devices
    - Novel boundary conditions

NEMO can trade of CPU time and memory against a variety of models.

All of NEMO's Facets: Formalism, Physics, and Technology

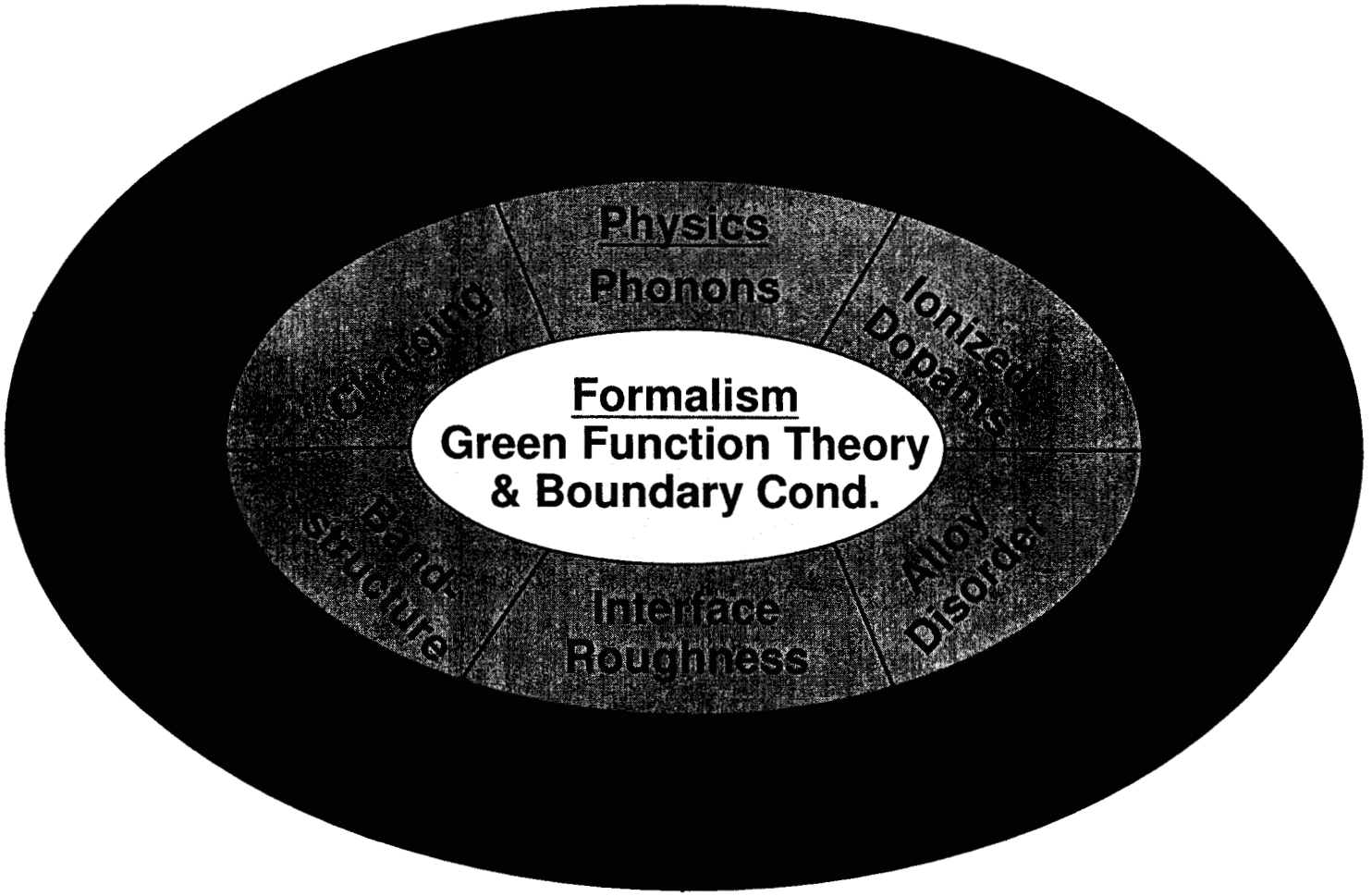

Approximately 250,000 lines of code at time of delivery

JPL

"Genetically Engineered" Nanoelectronic Devices

Objective:

- Automated device synthesis and analysis using genetic algorithms.
- Material spectroscopy through genetic algorithms analysis.

Justification:

- Empirical Design (usual process) is sub-optimal. Complete design space search is unfeasible.
  => Develop automated design tools.

Impact:

- Rapid nanotechnology device synthesis and development.
- Generation of novel devices.

Approach:

- Augment NEMO to analyze individual structures in parallel.
- Augment parallel genetic algorithm package (PGApack) to optimize and select desired structures in NEMO.

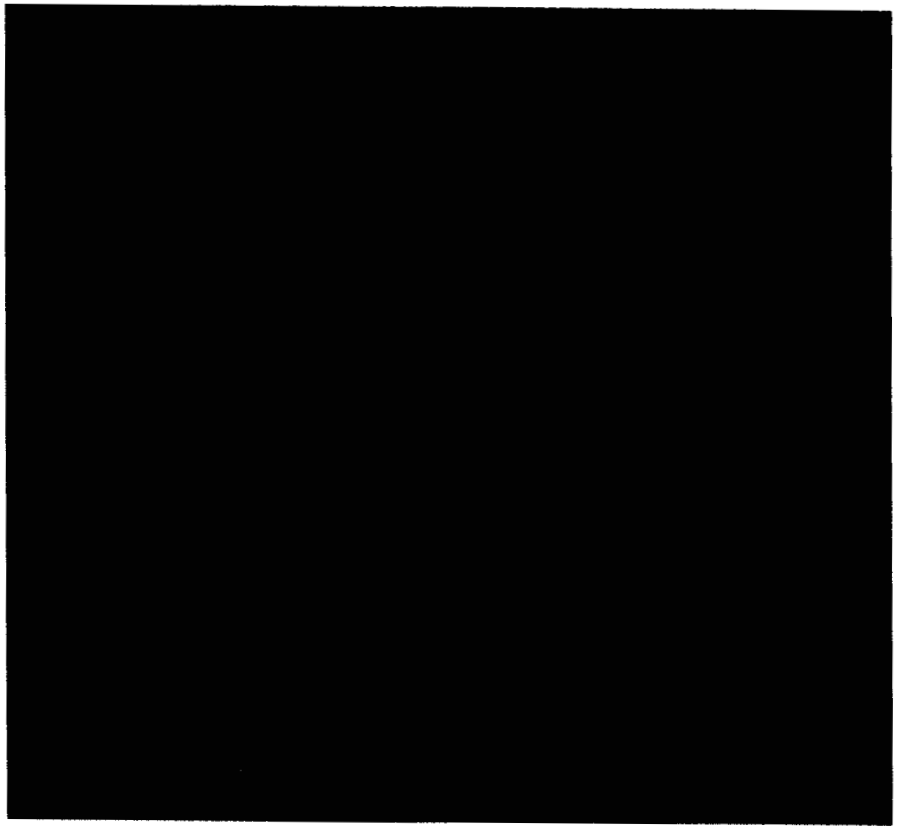

Proposed system architecture.
Prototype is operable in batch mode.

First Simulation Results: Structural Analysis

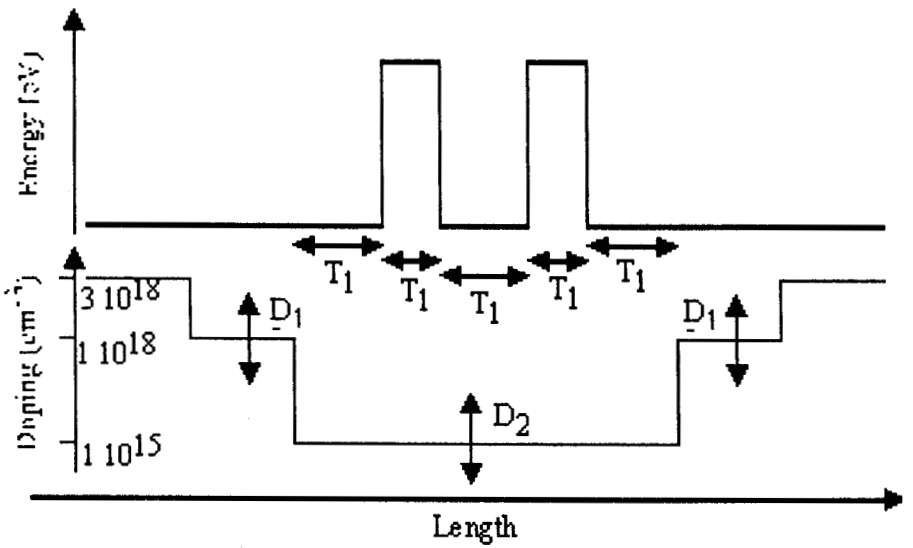

- Allow genetic algorithm to vary 5 different structural parameters:
  - 3 Thicknesses: well, barrier, spacer
  - 2 Dopings: low doped spacer, unintentional doping in center
- Employ parameterized non-parabolic single band model with full quantum charge self-consistency and transverse momentum integration.
- Developed fitness function for typical RTD I-V curves. Need to shoot for peak position and amplitude, slope at peak and relative and absolute errors.

First Simulation Results: Structural Analysis

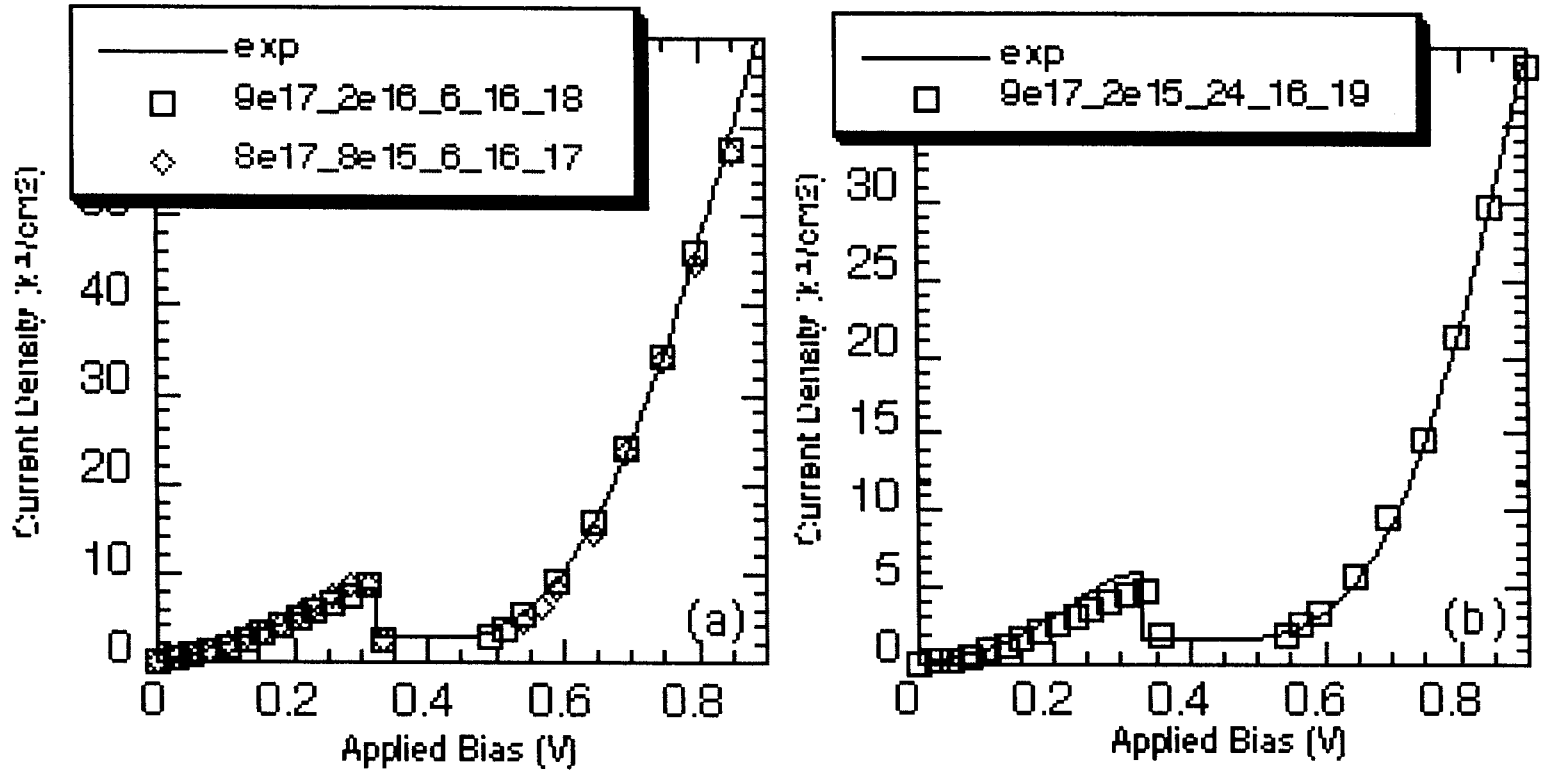

- Analyzed two similar InGaAs/InAlAs structures :
  - RTD 1: D1=1e18/cm^3, D2=1e15/cm^3, T1=7ml, T2=16ml, T3=16ml
  - RTD 2: D1=1e18/cm^3, D2=1e15/cm^3, T1=20ml, T2=16ml, T3=16ml

Future Interest

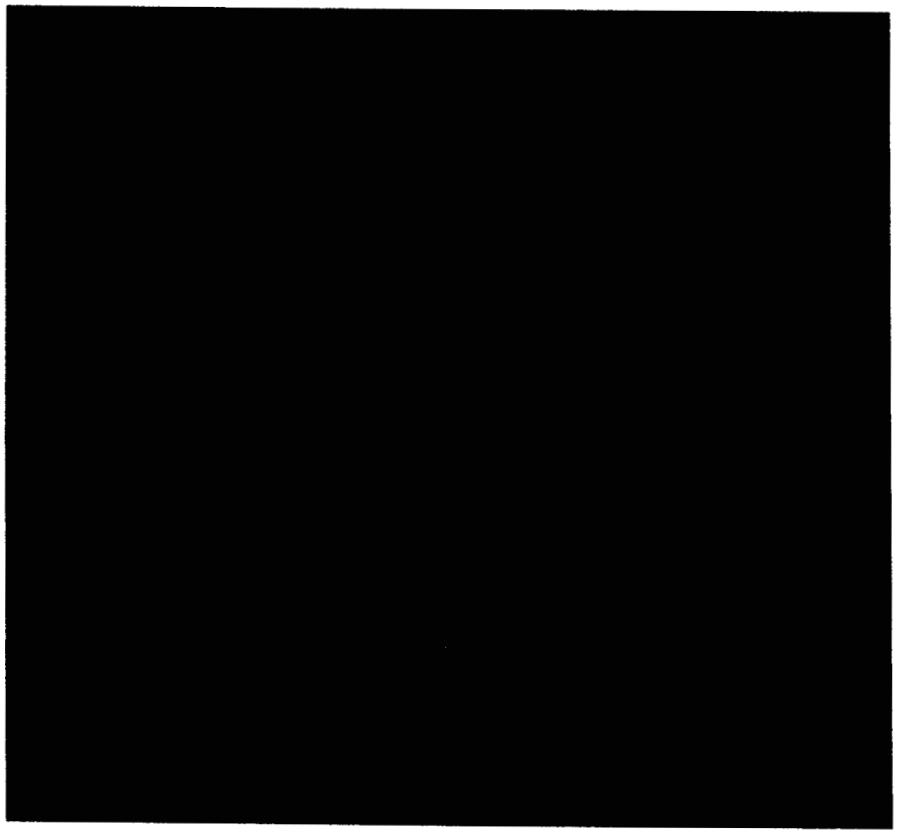

- Analyze material parameter influence on overall device performance
  -> material spectroscopy

- Implement general architecture such that a variety of different simulation tools can be plugged into an optimization tool.

- Explore other optimization algorithms, such as simulated annealing or directive approaches within the same framework.

  -> scripting tools that can link different tools

  -> Tcl/Tk

Outline

- NEMO genealogy and general features
- Structural device optimization:
  - Massively parallel genetic algorithm package
- Full band transport simulations:
  - Electron transport
  - Hole transport
- Comparison between k.p and sp3s*
- Conclusion

Transport via Transmission Coefficients

$$I \propto \int dk_x \int dk_y \int dE T\left(E, k_x, k_y\right)\left(f_L(E) - f_R(E)\right)$$

↓ Cylindrical Coordinates

$$I \propto \int d\varphi \int k dk \int dE T\left(E, k, \varphi\right)\left(f_L(E) - f_R(E)\right)$$

↓ Throw out angular dependence

$$I \propto 2\pi \int k dk \int dE T\left(E, k\right)\left(f_L(E) - f_R(E)\right)$$

↓ Parabolic transverse subbands

$$I \propto \rho_{2D} \int T(E)\left(f_L(E) - f_R(E)\right)$$

Full Band Simulation of RTD Electron Transport

- Mechanics of an energy E and transverse momentum k integration.
- Unphysical effects when parabolic subbands are assumed:
  - Overshoot at RTD turnoff.
  - Spurious bistability in charge self-consistent simulation.
- Transverse subbands.
- Full band simulation eliminates these spurious simulation effects.

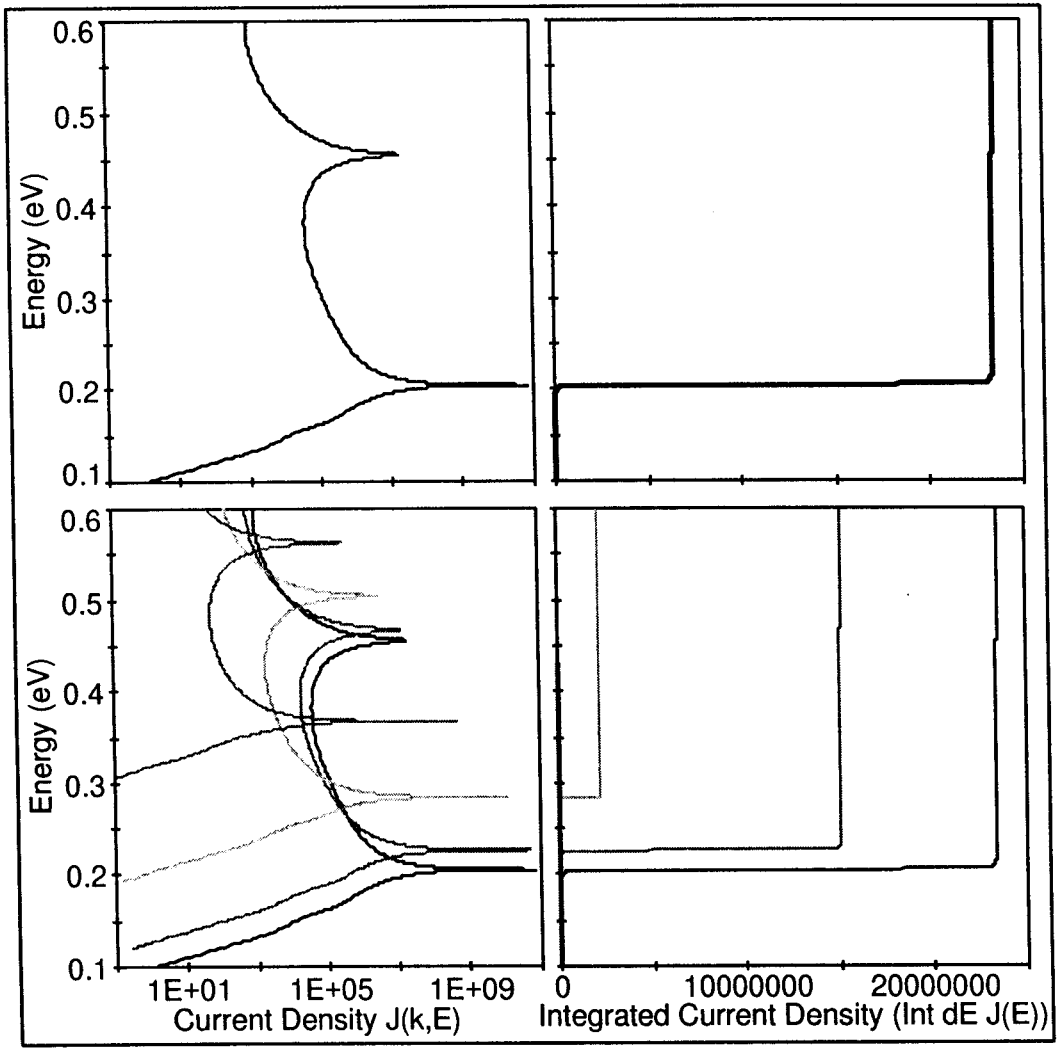

Mechanics of 2D Integration

- Transmission coefficient is masked by Fermi distribution in injecting lead.
- Running sum integral points out where in energy space significant current contributions occur.
- Multiple instead of a single transmission coefficient are evaluated and summed up.

$$J(E',k) \qquad \int_{-\infty}^{E} dE' J(E',k)$$

Mechanics of 2D Integration

- Transmission coefficient is masked by Fermi distribution in injecting lead.
- Running sum integral points out where in energy space significant current contributions occur.
- Multiple instead of a single transmission coefficient are evaluated and summed up.

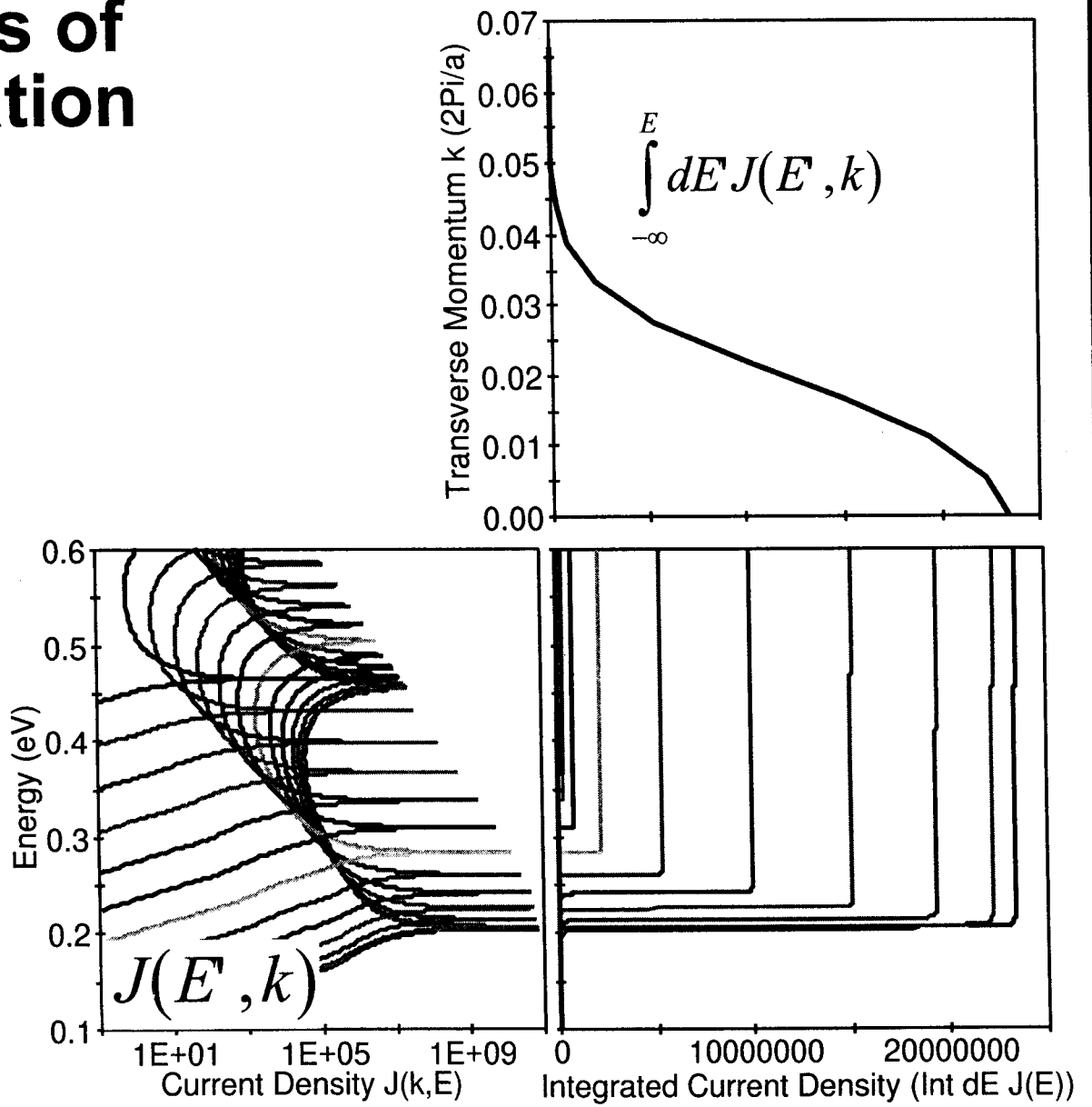

Full Band Simulation of Electron Transport

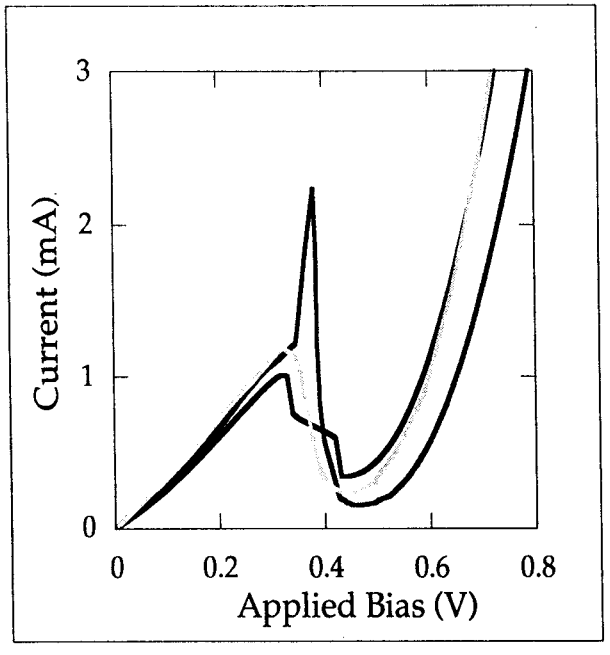

InGaAs/InAlAs V1909 #4

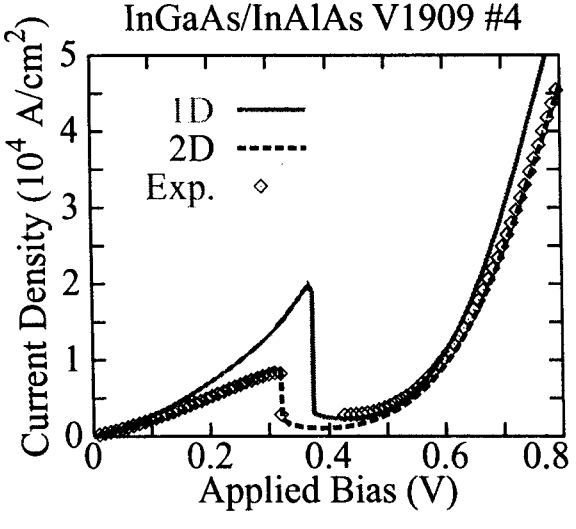

- 1D integration assuming parabolic subbands can lead to unphysical current overshoots.
- 2 Examples on InGaAs/InAlAs simulations:
  - Sp3s* simulation with partial charge self-consistency -> sharp spike at turn-off
  - Parameterized single band simulation which incorporates the band-non-parabolicity -> overall current overshoot.
- -> 2D integration fixes these unphysical results.

Resonance Coupling vs. Transverse Momentum

Density of States (k_x=0.00)

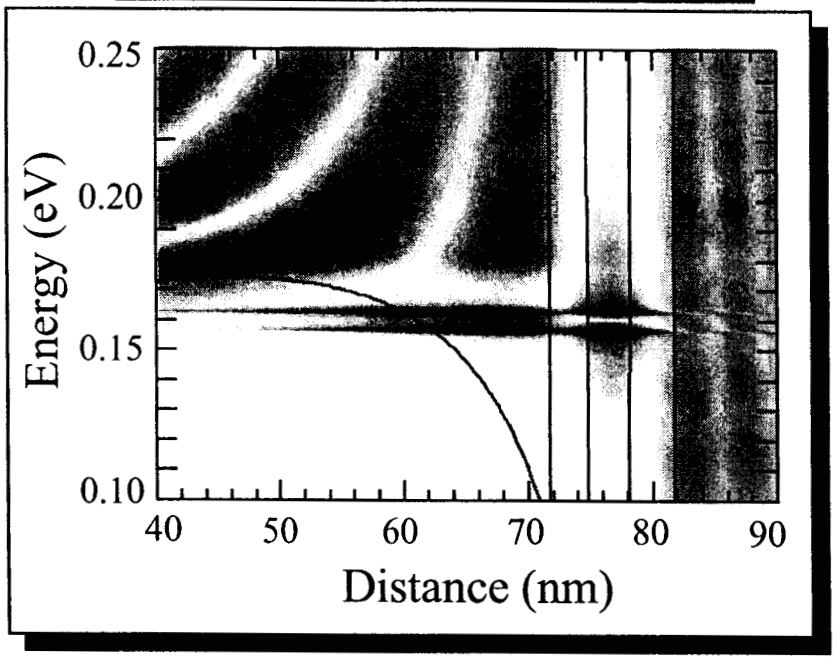

Density of States (k_x=0.03)

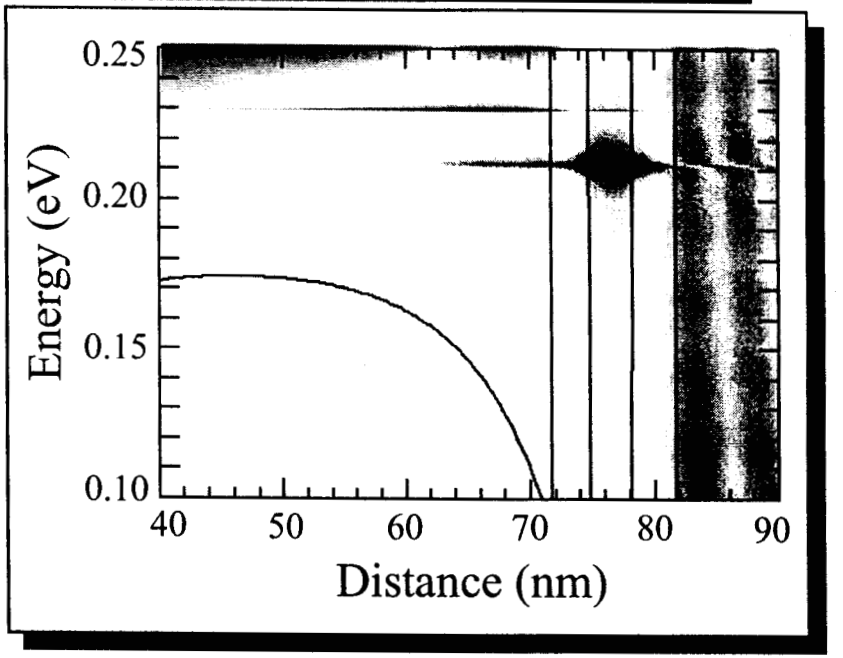

Resonance coupling depends on the transverse momentum

Quantum Well and Notch Subbands

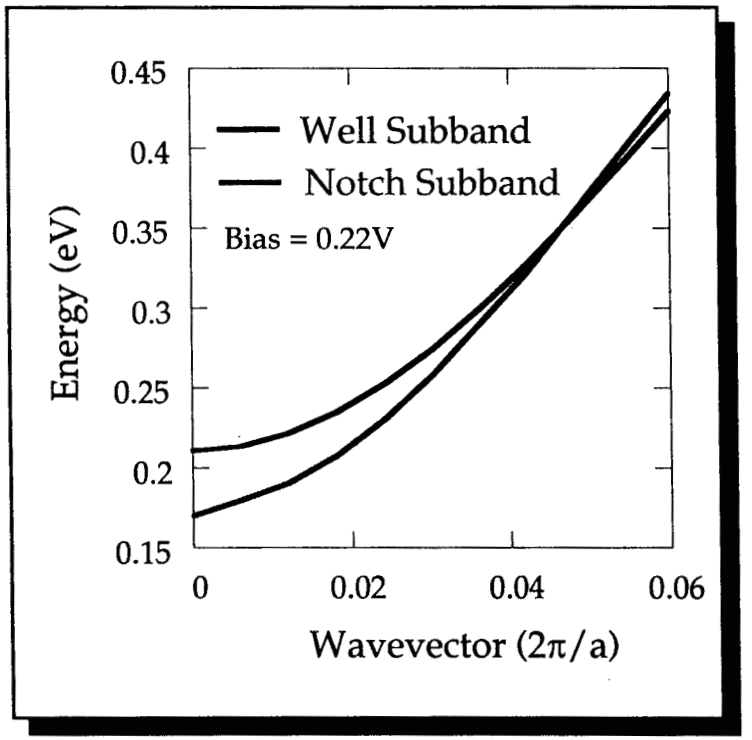

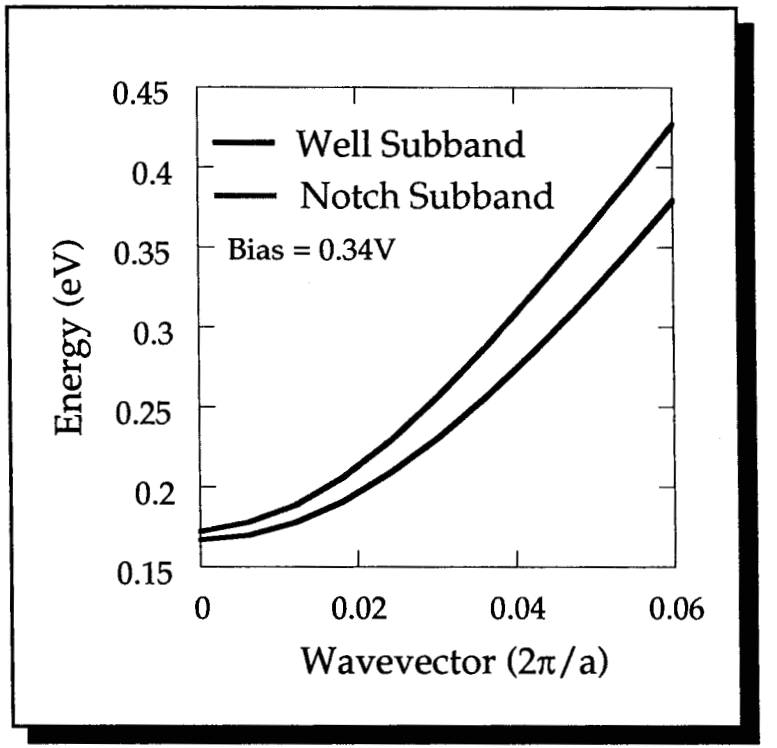

- The dispersions are non-parabolic
- There is no "perfect" overlap of the subbands

Spurious Bistability

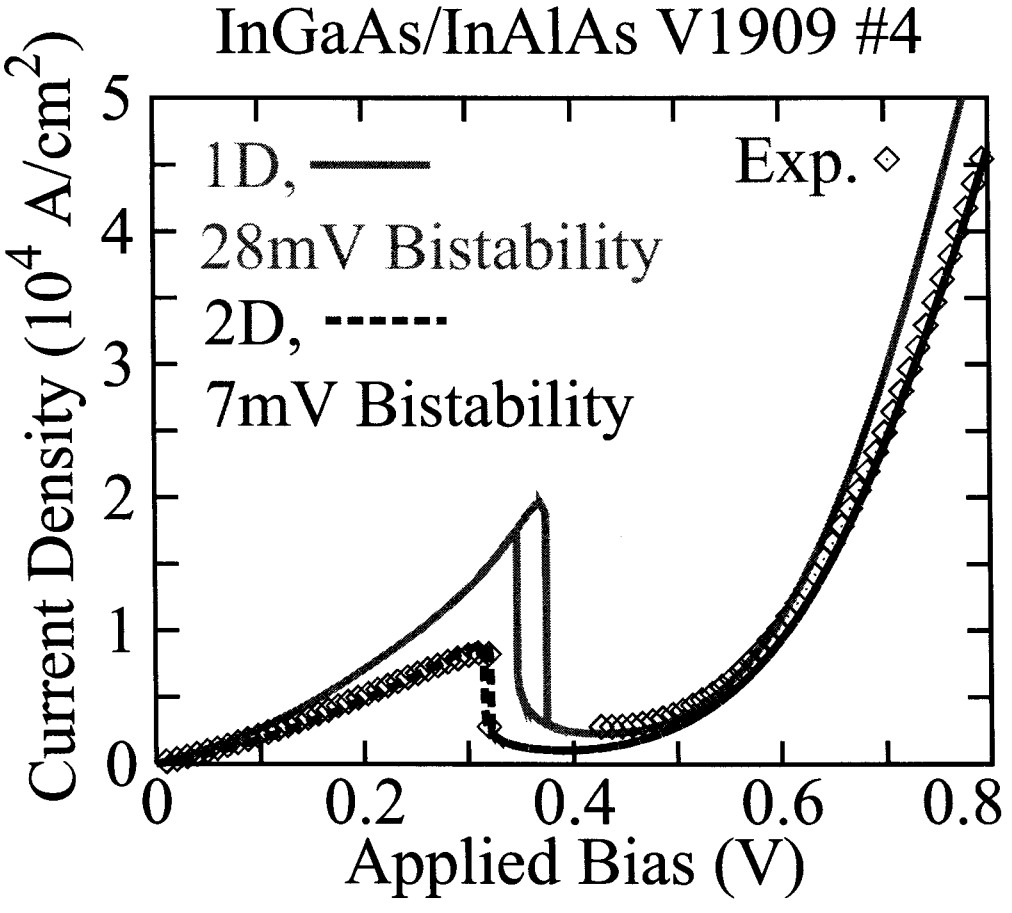

- **Most quantum charge self-consistent simulations of RTD's exhibit a bistability in the NDR region when the simulation is performed in a reverse voltage sweep.**
- **This is (we believe) a numerical artifact and typically not observed in experiments.**
- **Full band integration reduces the spurious bistability significantly.**

JPL

Effect of Exchange and Correlation Potential

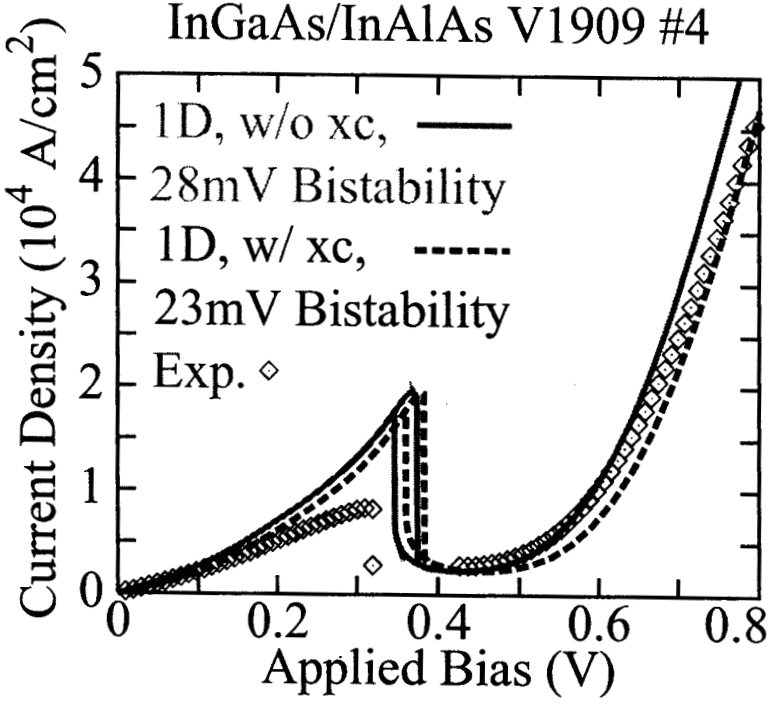

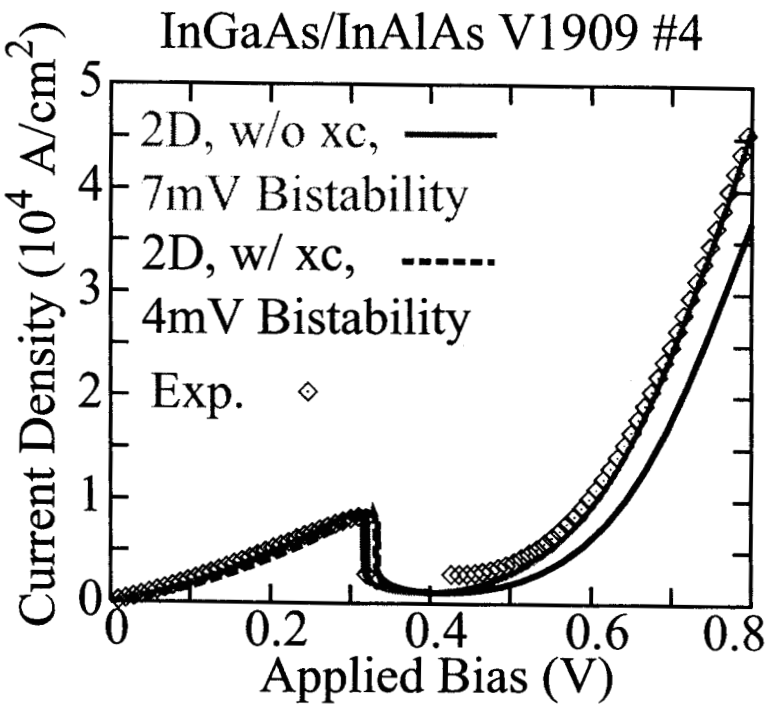

- **Calculate the exchange and correlation potential in the local density approximation.**
- **Exchange and correlation energy does not eliminate (in general) the bistability, it does reduce it however.**
- **Inclusion of scattering in the simulation reduces the bistability region as well.**

Outline

- NEMO genealogy and general features
- Structural device optimization:
  - Massively parallel genetic algorithm package
- Full band transport simulations:
  - Electron transport
  - Hole transport
- Comparison between k.p and sp3s*
- Conclusion

JPL

Hole Transport in a AlAs/GaAs/AlAs RTD

- Resonance states
- Transverse momentum subbands
- Need for energy and transverse momentum integration
- Current flow away from zone center
- Dependence on the direction of the transverse momentum (<100> vs. <110> integration).

JPL

GaAs Bulk HH and LH Bandstructure

Computed in second nearest neighbor sp3s* tight binding model with explicit spin (20x20 basis).

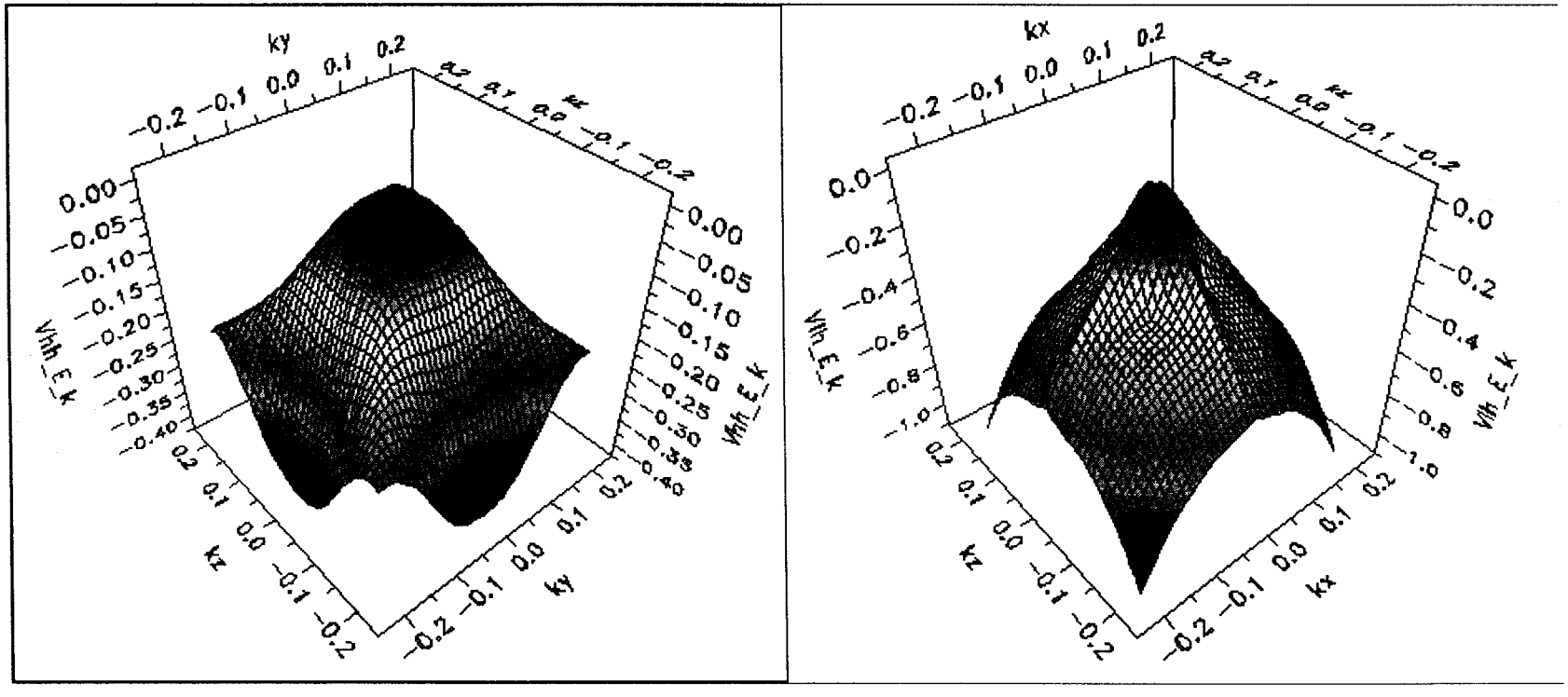

Heavy holes heavier in <110> than <100>

$m_{110} > m_{100}$

Light holes lighter in <110> than <100>

$m_{110} < m_{100}$

JPL

Hole Resonance States in GaAs/AlAs RTD

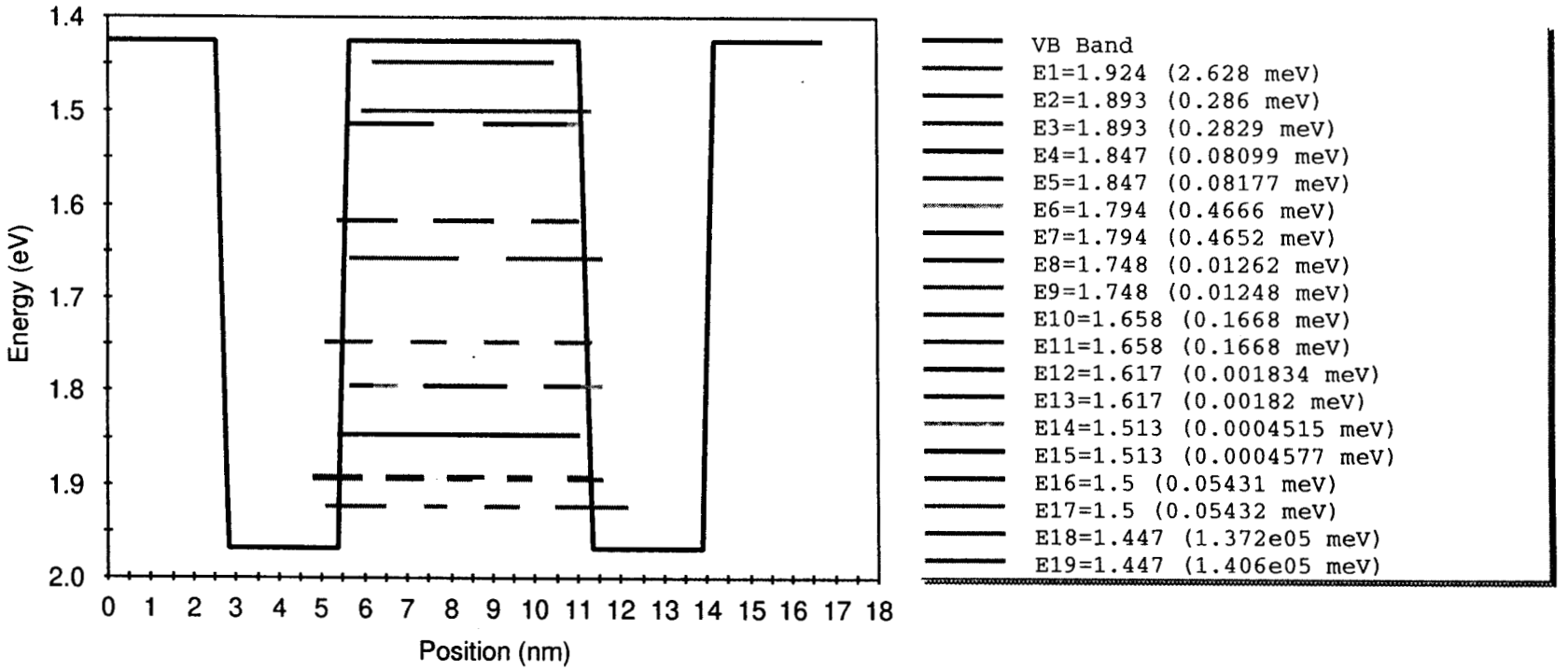

- Look at simple structure:
  - 10 monolayer AlAs barriers
  - 20 monolayer GaAs well
  - Flat band conditions
- Use 2nd nearest neighbor sp3s* tight binding model
- Compute resonance energies and resonance linewidths using a order N non-hermitian matrix eigenvalue solver

Hole Transport in a GaAs/AlAs RTD

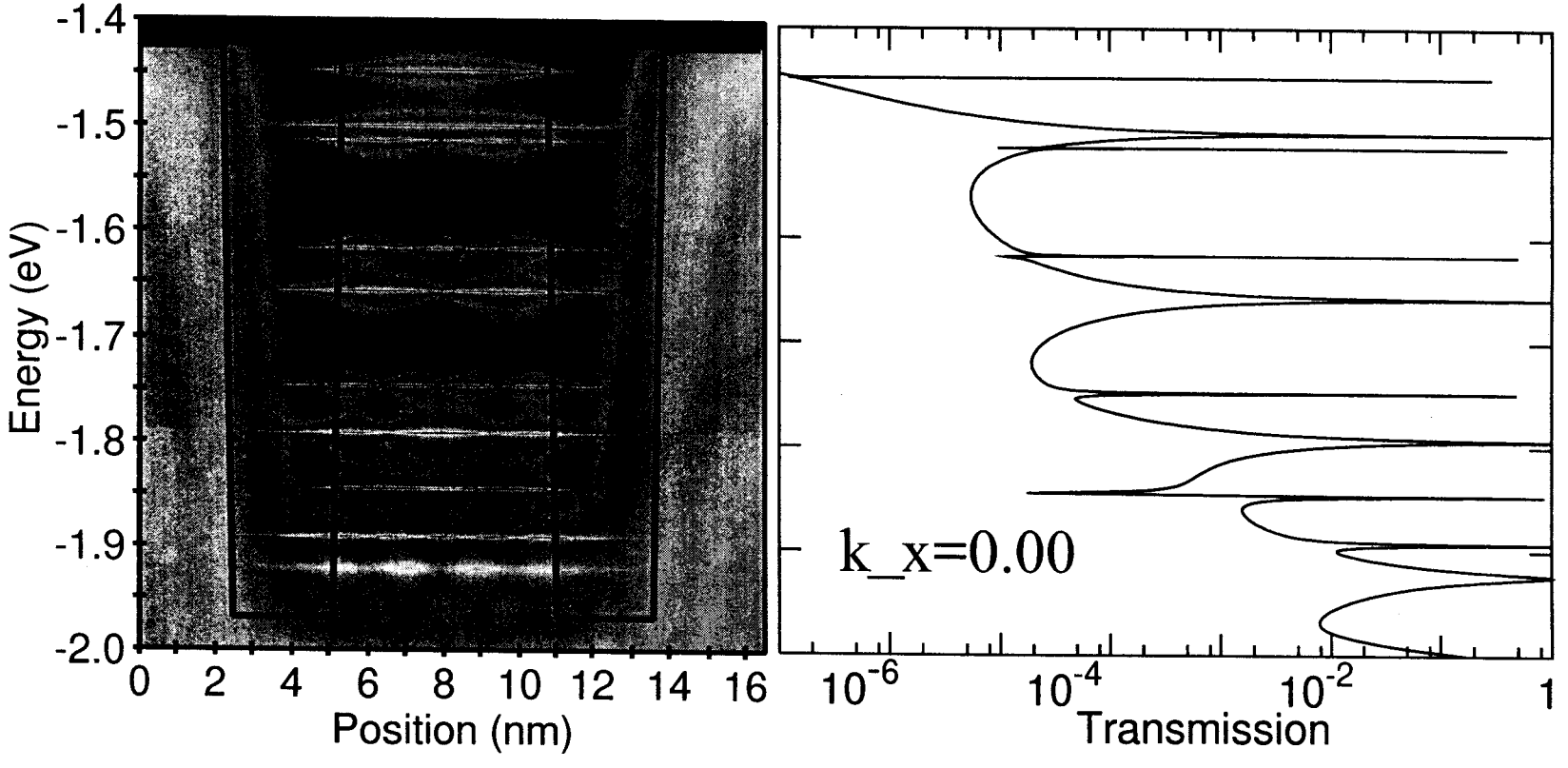

- **Density of states (DOS):**
  - **Low DOS - Dark (blue) tones**
  - **High DOS - light (red) tones**

- **Transmission coefficient at k_x=0**
  - **Light hole states strongly coupled to continuum -> wide resonances**
  - **Heavy hole states weakly coupled to continuum->narrow**

Transverse Hole Subbands in GaAs/AlAs RTD

- Transmission coefficient at $k_x=0$
- Resonance states as a function of transverse momentum: -> transverse subbands
- Transmission coefficient at $k_x=0.05$

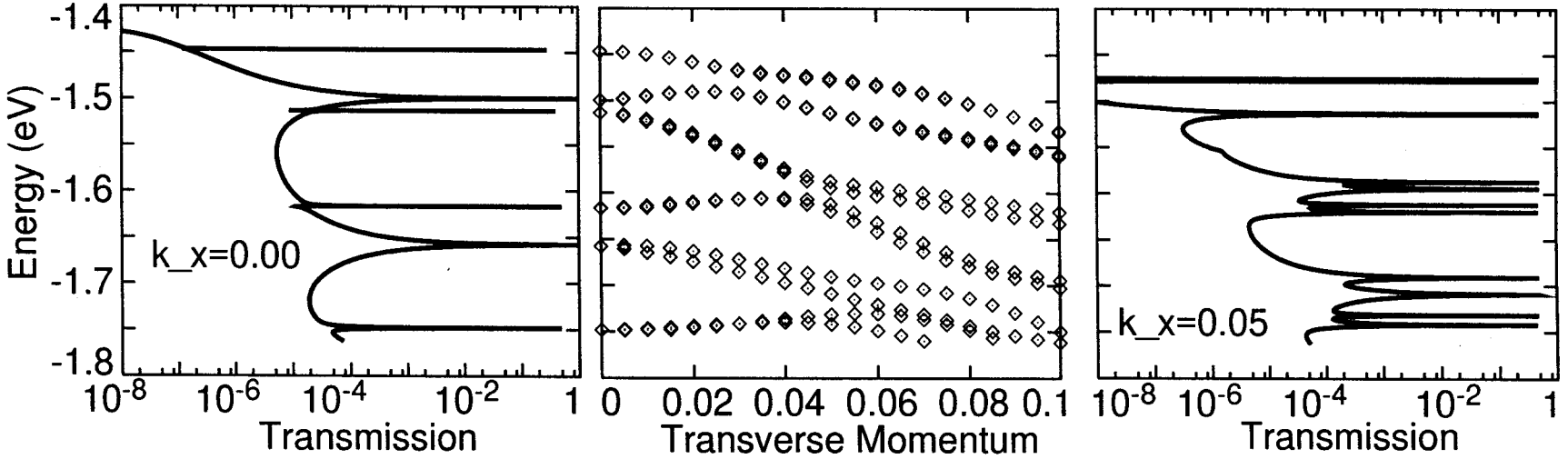

- Transverse subbands exhibit:
  - complex structure of anti-crossings
  - Non-monotonic behavior - some subbands are electron-like.

- Why do some of the subbands increase in energy?

Excited HH-States Move up in Energy

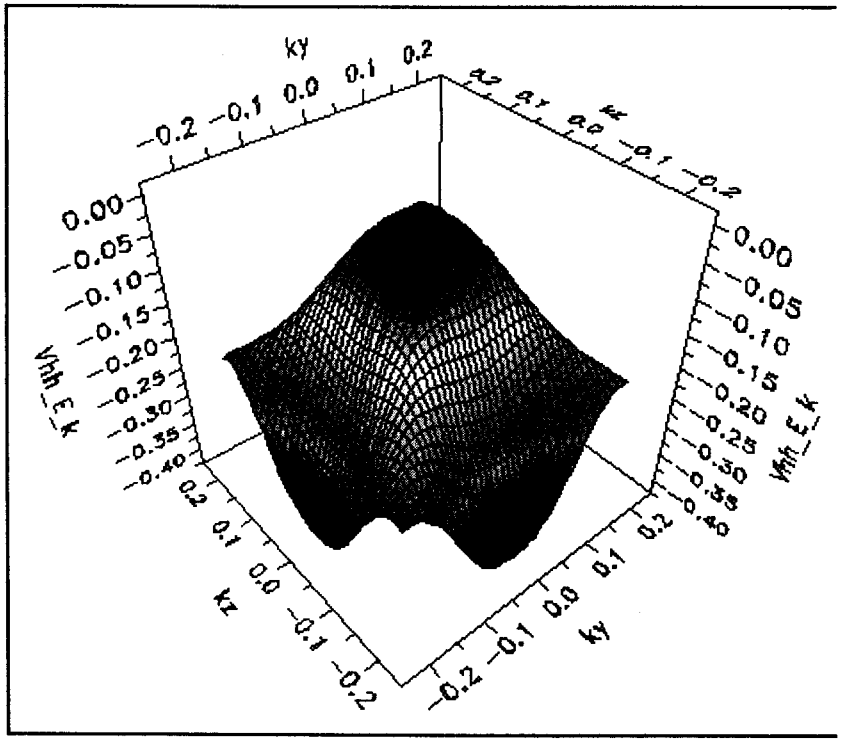

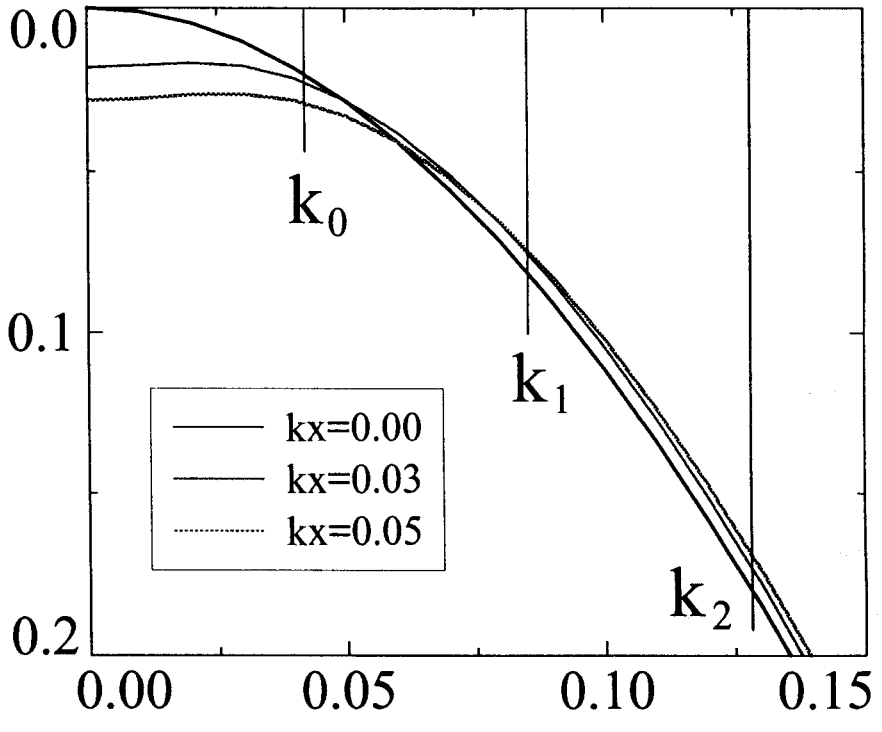

- HH Bulk dispersion in (k_x,k_y,0.0) shows strong anisotropy in <100> vs. <110> direction.

- Slice (k_x,k_y,0.0) surface for 3 different k_x (black, blue, and red curve).
- k_0 indicates the heavy hole ground state determined by ~π/L
- $k_1=2k_0$: first excited state - moves up
- $k_2=3k_0$: second excited state - moves up

LH-States Move down in Energy

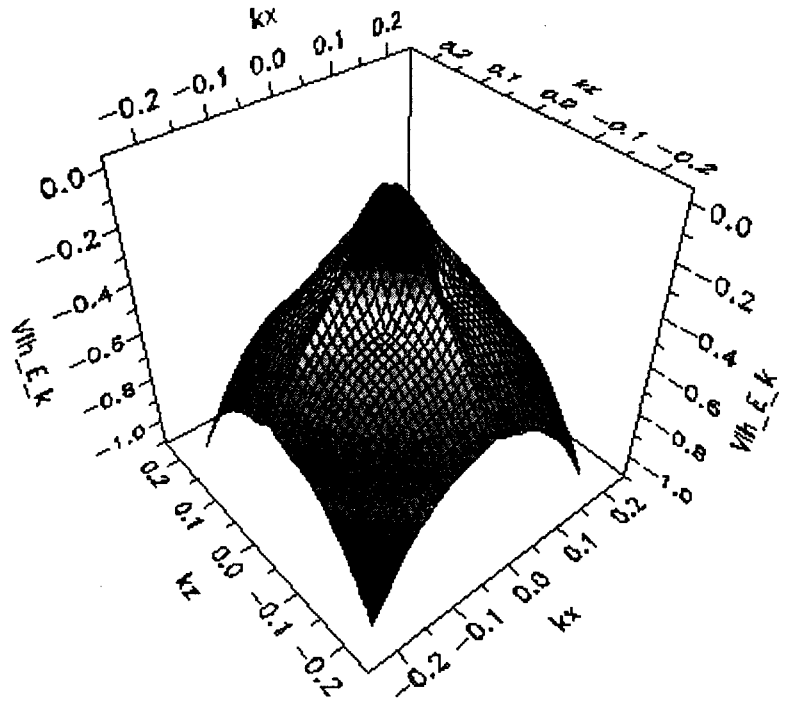

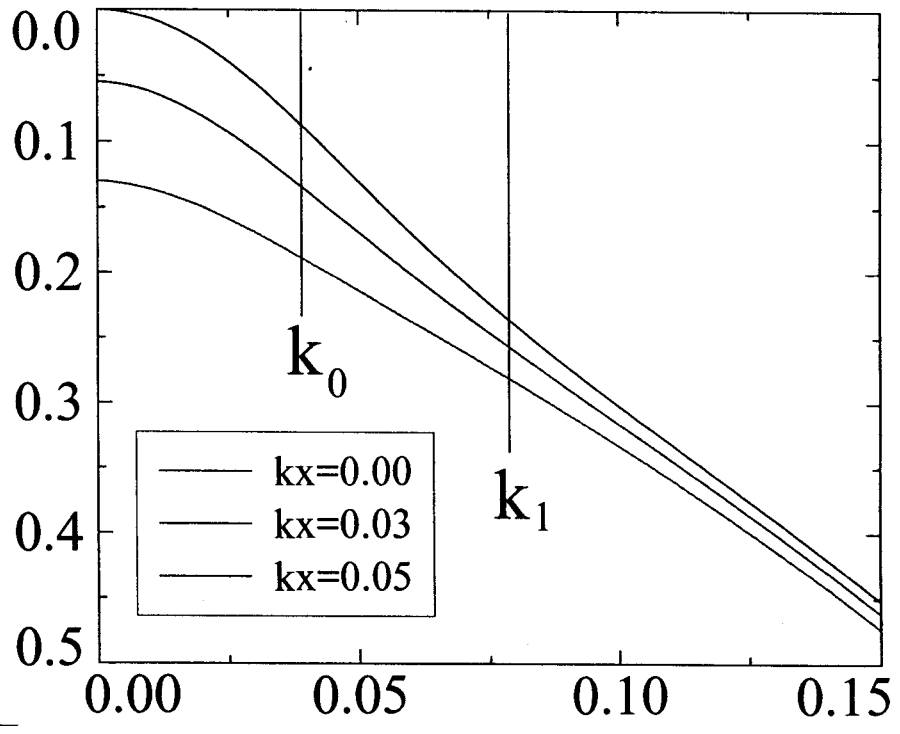

- HH Bulk dispersion in (k_x,k_y,0.0) shows strong anisotropy in <100> vs. <110> direction.

- Slice (k_x,k_y,0.0) surface for 3 different k_x (black, blue, and red curve).
- k_0 indicates the light hole ground state determined by ~π/L ground state moves down fast
- $k_1=2k_0$: first excited state moves down

Cave Canem!
Beware of the Wolf!

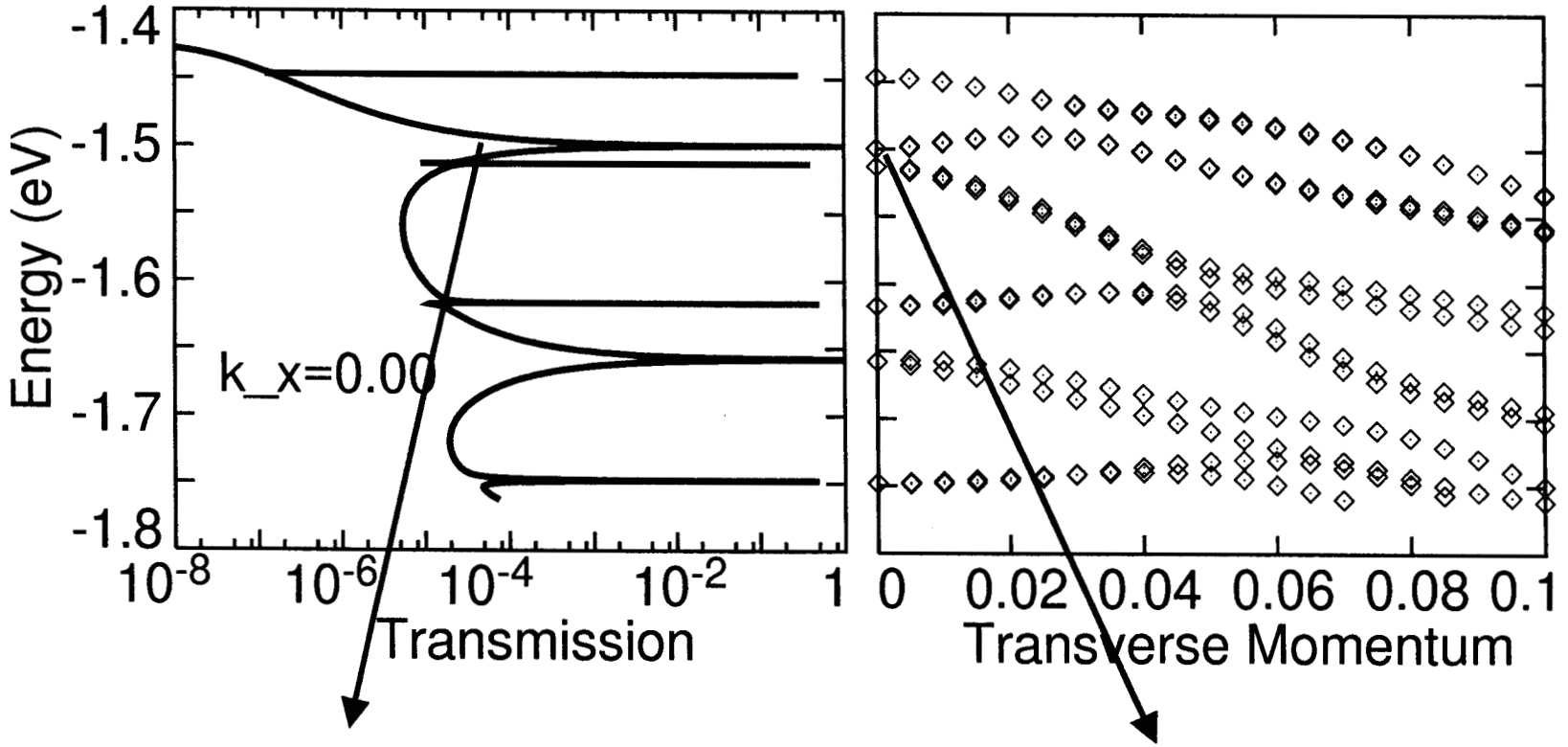

- What looks like a light hole resonance with a neighboring heavy hole resonance is already a strongly mixed state
- Observe an anticrossing of two states at $k_x=0$

More Latin: nemo = nobody

Narrow GaAs Well

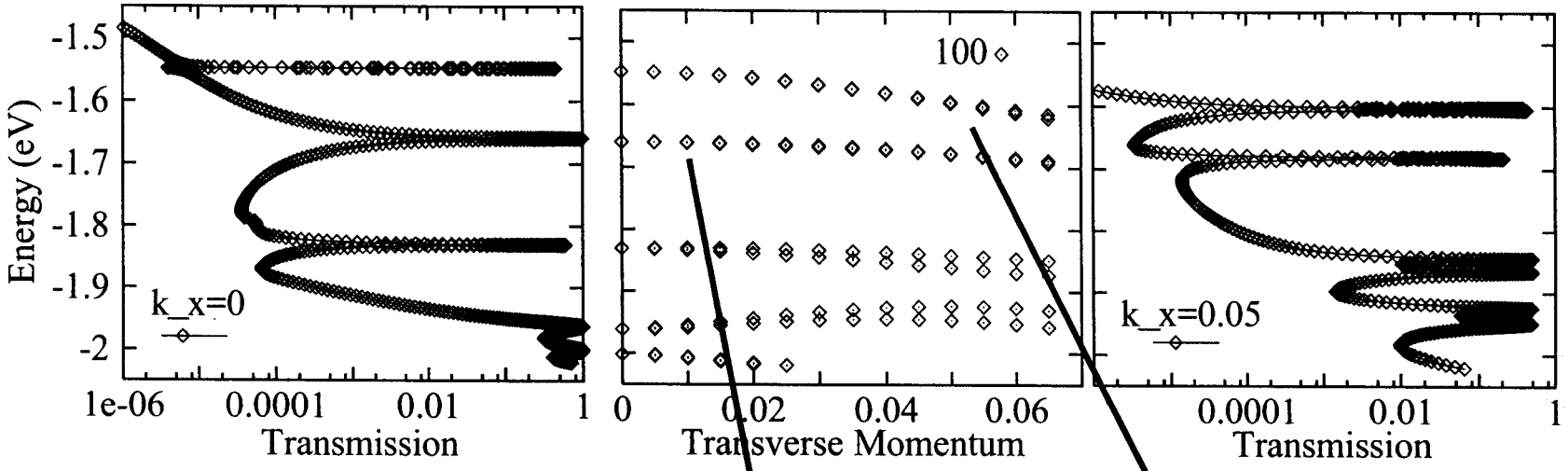

- **AlAs/GaAs/AlAs structure,10/07/10 ml thickness**
- **LH1 at k_x=0 is de-coupled from HH2 due to strong confinement**

LH dispersion is almost flat

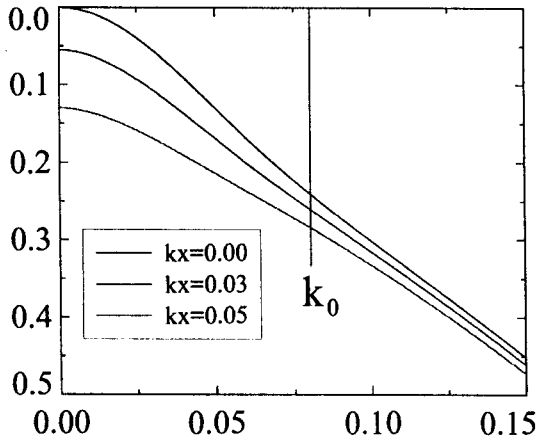

LH1 at k_x=0.05 anti-crosses with HH1

Hole Transport

$$I \propto \int dk_x \int dk_y \int dE T\left(E, k_x, k_y\right)\left(f_L(E) - f_R(E)\right)$$

↓ **Cylindrical Coordinates**

$$I \propto \int d\varphi \int k dk \int dE T\left(E, k, \varphi\right)\left(f_L(E) - f_R(E)\right)$$

↓ **Throw out angular dependence**

$$I \propto 2\pi \int k dk \int dE T\left(E, k\right)\left(f_L(E) - f_R(E)\right)$$

↓ **Parabolic transverse subbands**

$$I \propto \rho_{2D} \int T(E)\left(f_L(E) - f_R(E)\right)$$

Current Integral Varies Qualitatively with Different Transverse Momenta

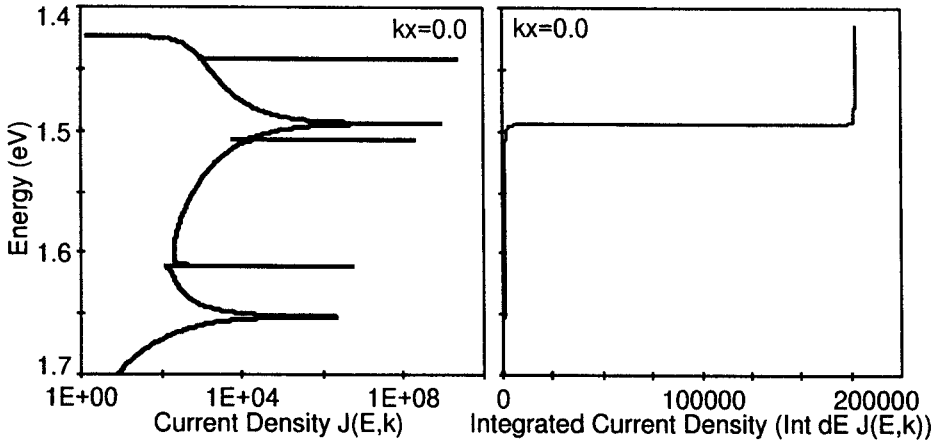

k=0.00:
current flows at one energy

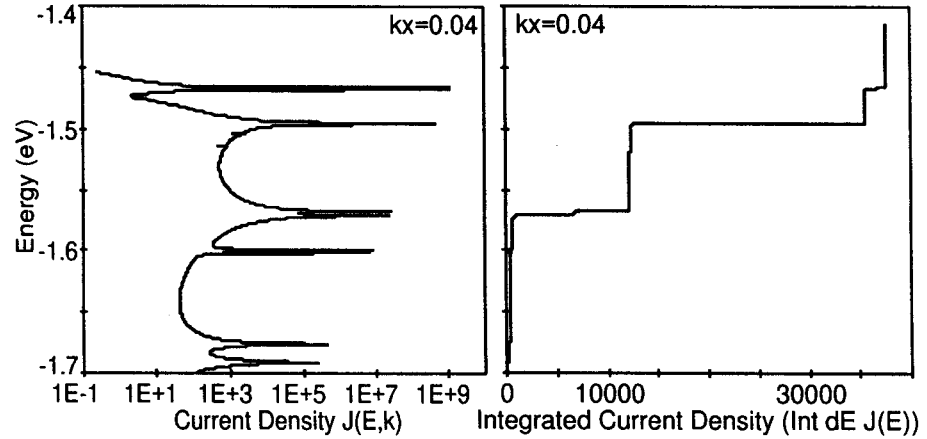

k=0.04:
current flows at multiple energies

$$J(E',k) \qquad \int_{-\infty}^{E} dE' J(E',k)$$

Current Density J(k)

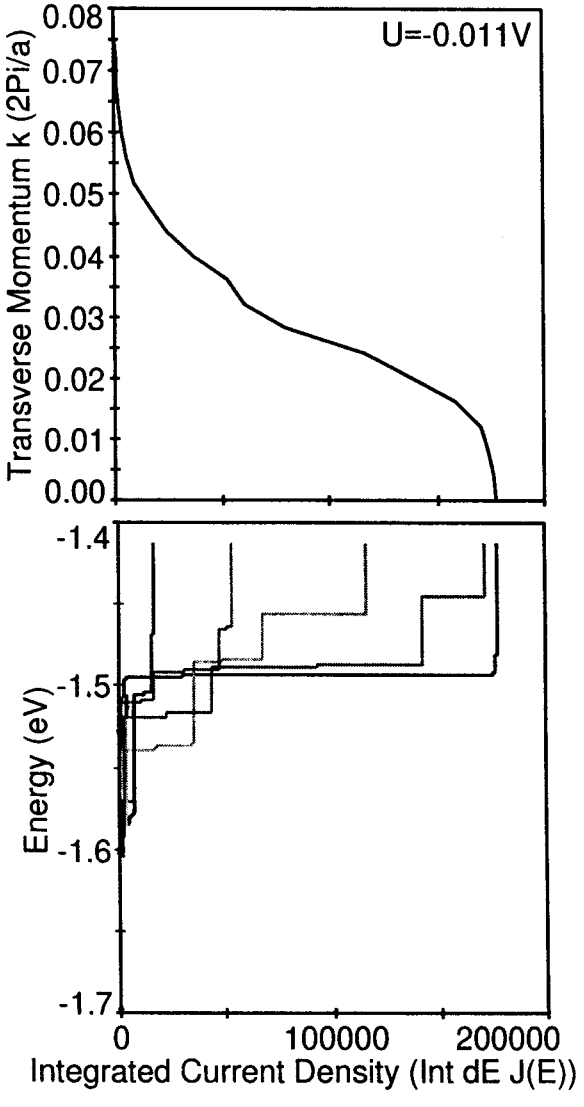

$$J(k) = \int_{-\infty}^{\infty} dE\, J(E,k)$$

- J(k) decreases with increasing k
- J(E,k) is widely distributed in energy

Current Voltage Characteristic

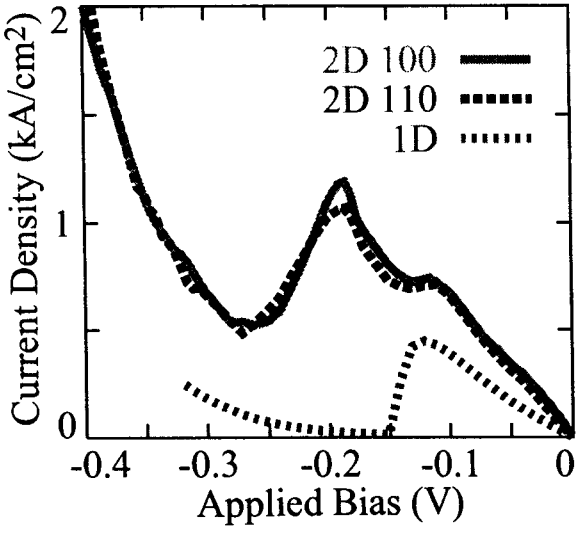

- Transverse integration provides qualitatively different results.
- Current dependence of k_t in <100> or <110> direction is weak.
- Current may be flowing dominantly outside the zone center.

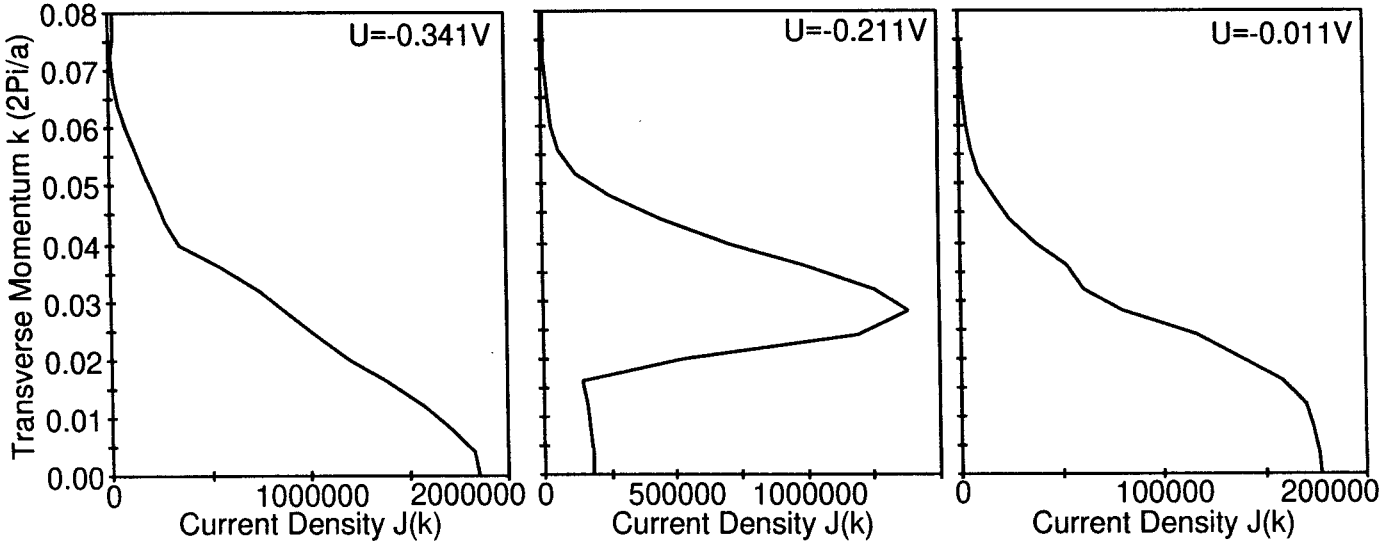

Outline

- NEMO genealogy and general features
- Structural device optimization:
  - Massively parallel genetic algorithm package
- Full band transport simulations:
  - Electron transport
  - Hole transport
- Comparison between k.p and sp3s*
- Conclusion

JPL

Comparison of GaAs sp3s* and k.p bulk bandstructure

- 3 Valence bands, 1 conduction band,
- k.p parameters such that bandgaps and effective masses are identical to tight binding

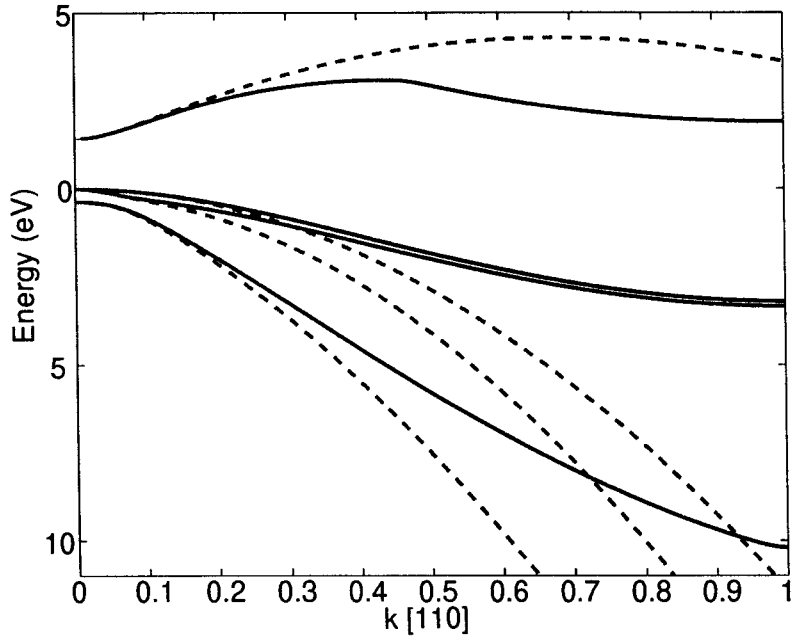

[100]

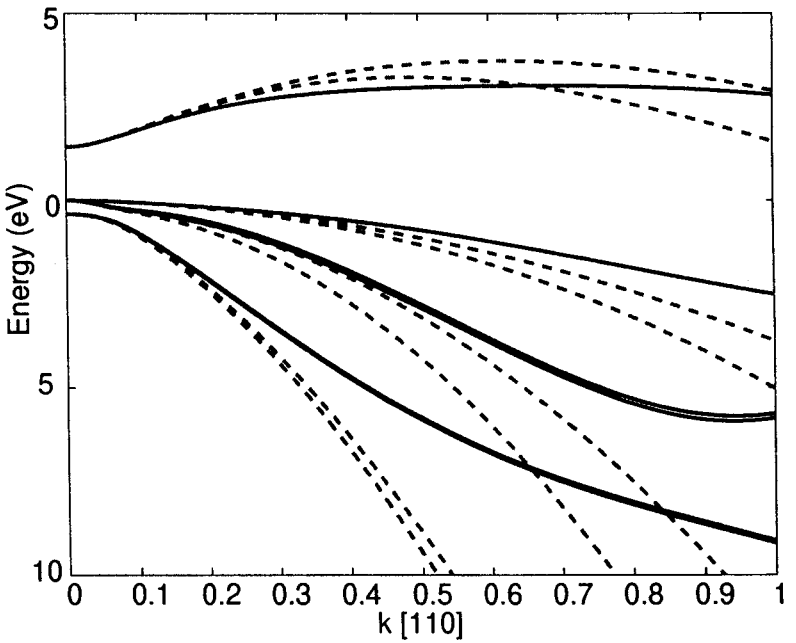

[110]

Comparison of GaAs sp3s* and k.p bulk bandstructure

- 3 Valence bands
- k.p parameters such that bandgaps and effective masses are identical to tight binding

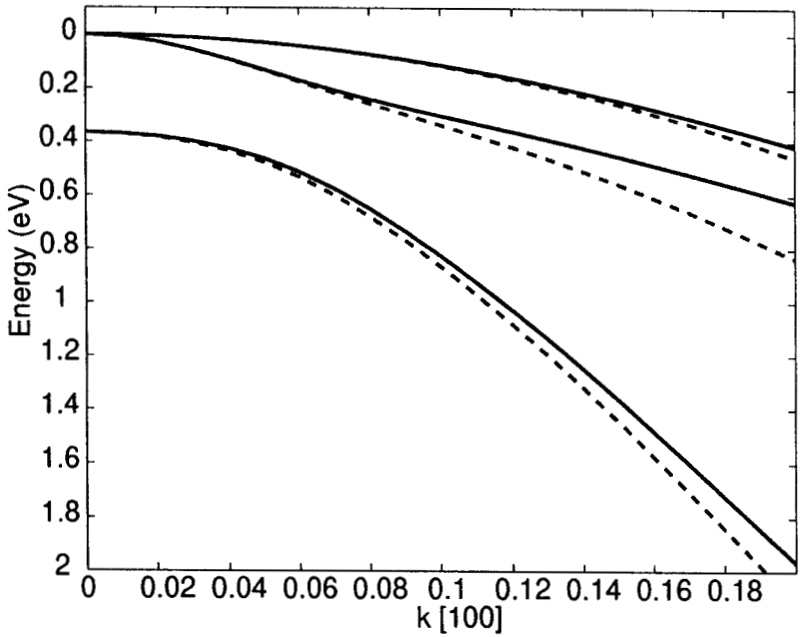

[100]

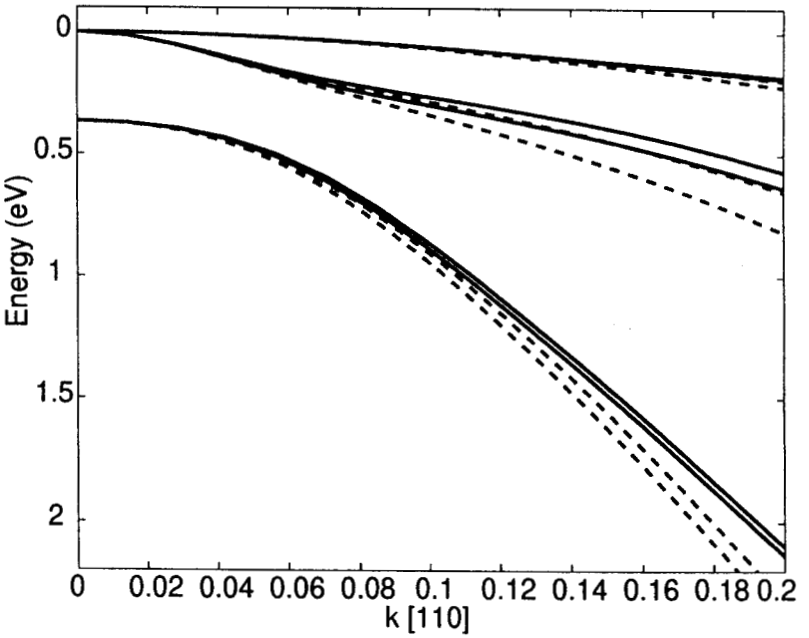

[110]

Comparison of GaAs sp3s* and k.p bulk bandstructure

- 1 conduction band
- k.p parameters such that bandgaps and effective masses are identical to tight binding

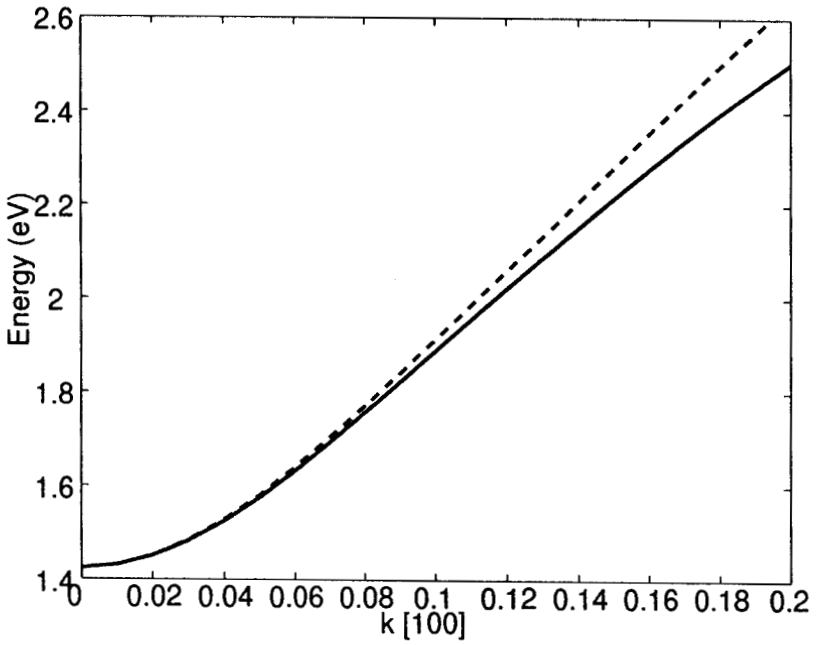

[100]

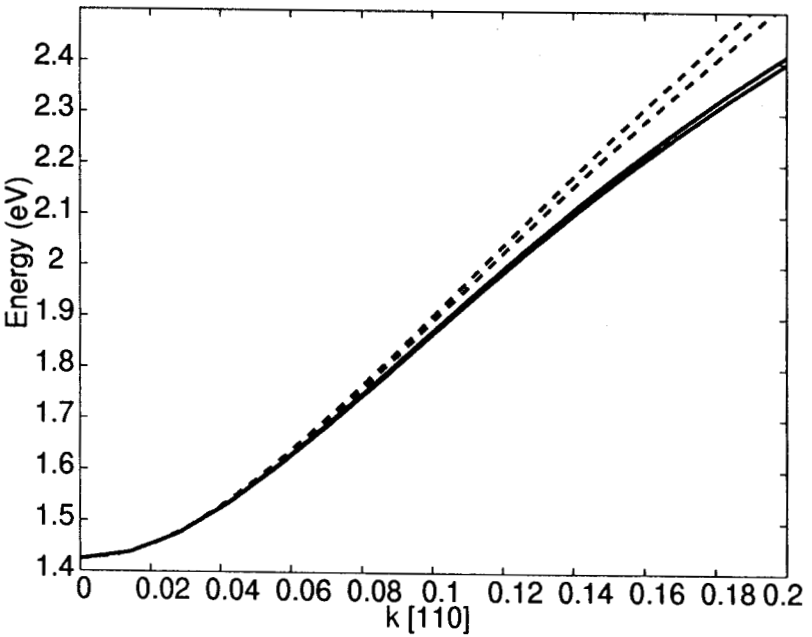

[110]

Sp3s* vs. k·p: Transverse Subbands in 30ml $Al_{0.3}Ga_{0.7}As/GaAs/Al_{0.3}Ga_{0.7}As$ Quantum Well

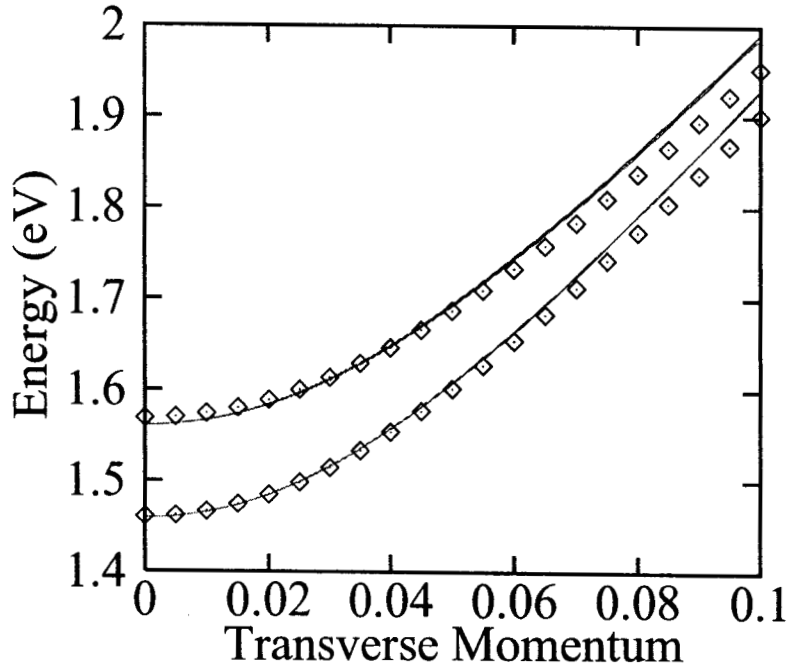

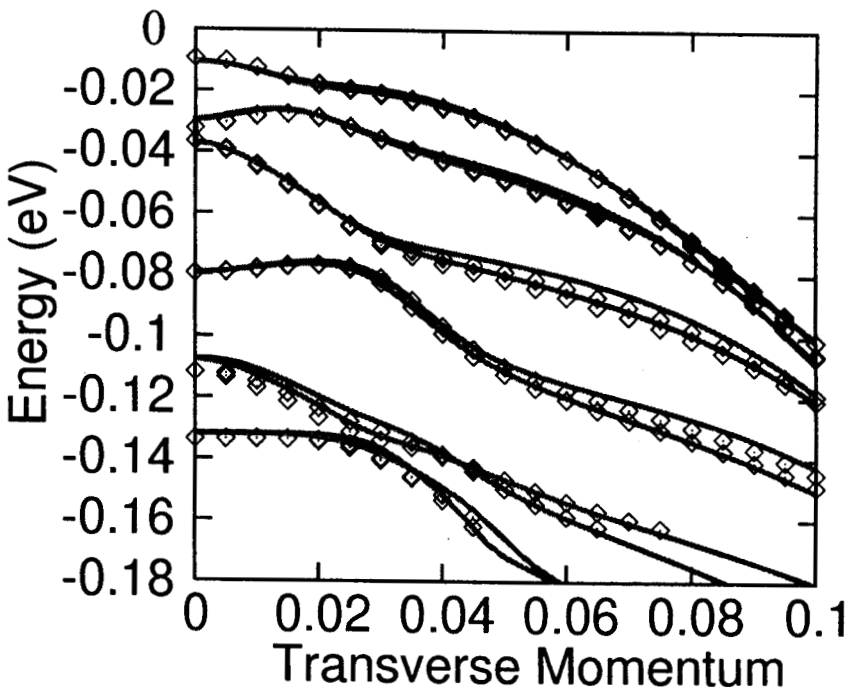

- Subbands in the [100] direction. Lines are k.p, dots are sp3s*.
- K.p parameters are adjusted to reflect sp3s* bandgaps and effective masses.

Comparison of InAs sp3s* and k.p bulk bandstructure

- 3 Valence bands, 1 conduction band,
- k.p parameters such that bandgaps and effective masses are identical to tight binding

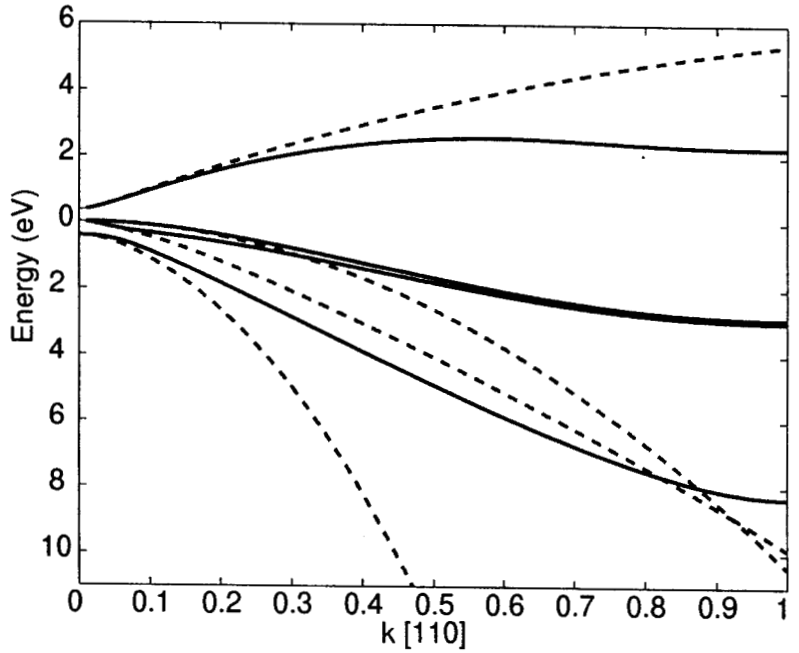

[100]

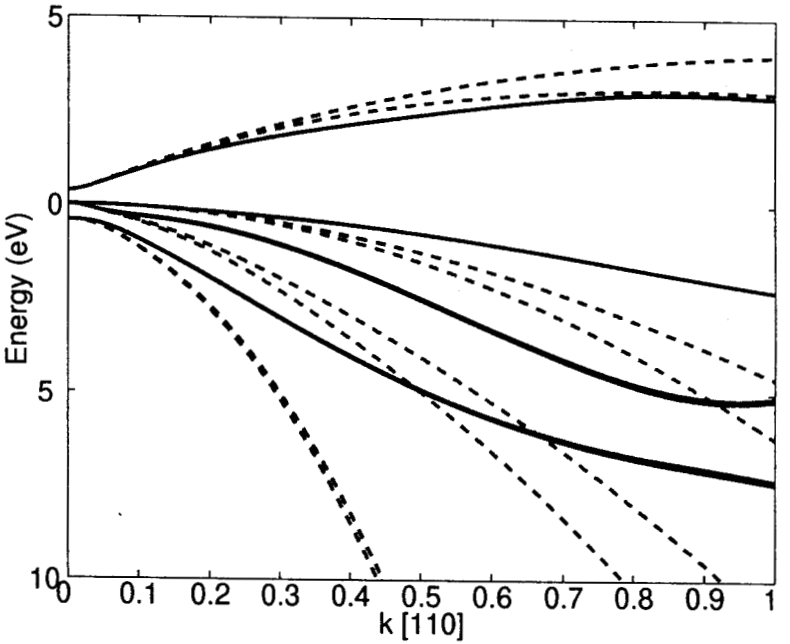

[110]

JPL

Comparison of InAs sp3s* and k.p bulk bandstructure

- 3 Valence bands
- k.p parameters such that bandgaps and effective masses are identical to tight binding

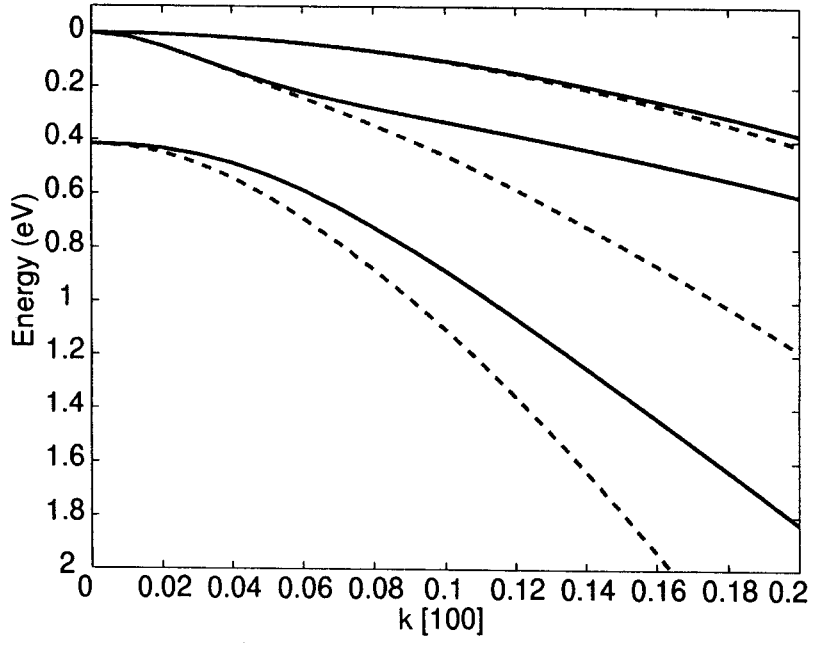

[100]

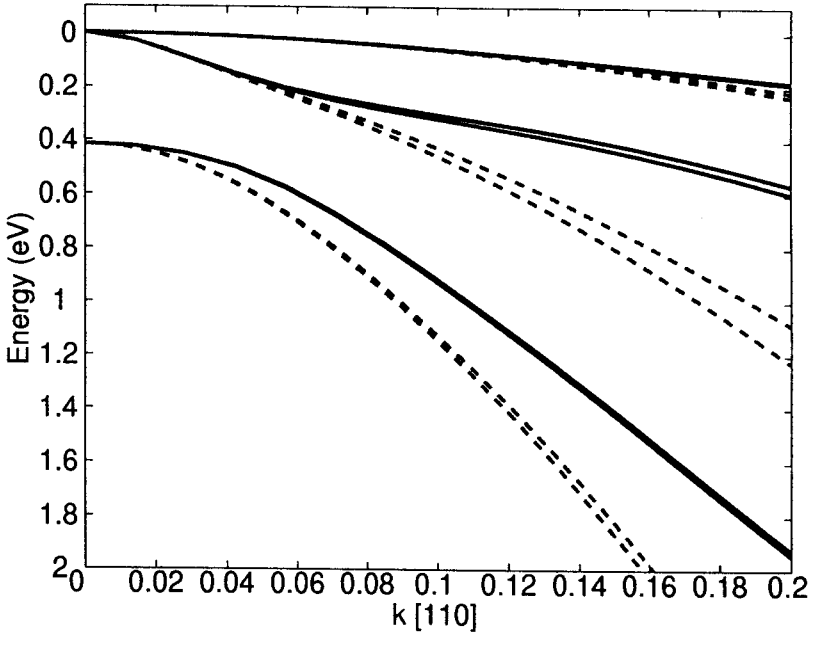

[110]

Comparison of InAs sp3s* and k.p bulk bandstructure

- 1 conduction band
- k.p parameters such that bandgaps and effective masses are identical to tight binding

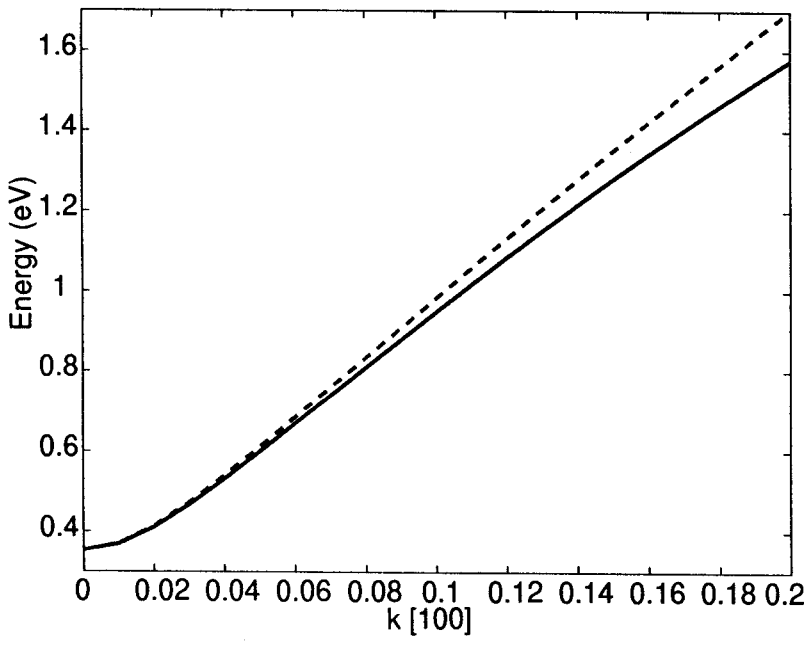

[100]

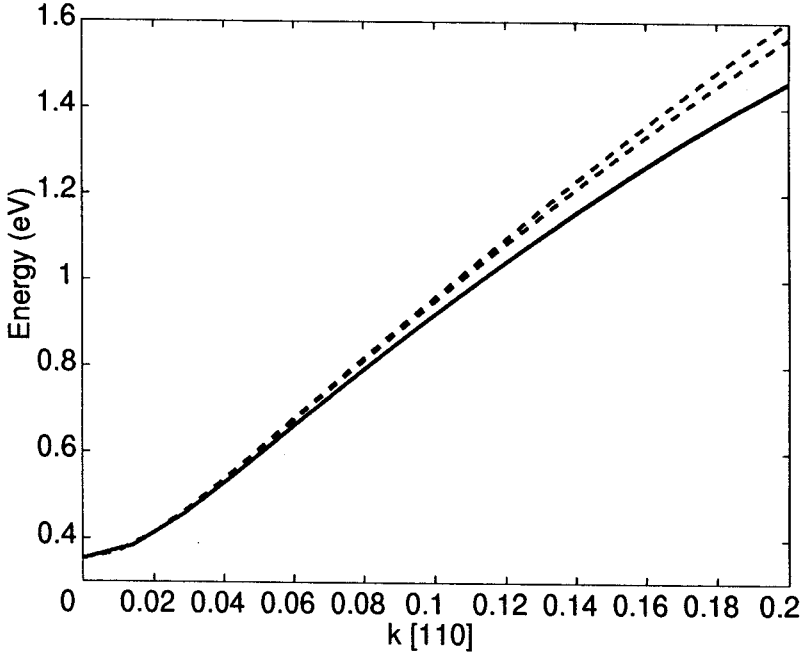

[110]

JPL

Open list for pros and cons: tight binding vs. k.p

- K.p better than tight binding:
  - Easier parameterization.
  - Faster simulations.

- Tight binding better than k.p:
  - Spatial discretization lends itself to incorporation of:
    - Space charge effects, arbitrary electrostatic potentials
    - Open boundary effects - real structures are typically non-periodic
    - Transport simulations (coherent and incoherent)
  - Transport away from zone center (Γ-X-Γ), indirect gap materials

- Both models fudge:
  - TB: adjust interactions to optimize the bands of interest
  - K.p: exclude higher bands from basis set and include their effects via Löwdin perturbation.

Conclusions

- Full band simulation is essential for:
  - Quantitative electron transport
  - Qualitative hole transport
- We will implement a discretized tight binding model into NEMO and evaluate the performance in transport simulation.
- Genetic algorithm was used to drive NEMO as a black box for structural optimization.